COBEM 2023 27TH INTERNATIONAL CONGRESS OF MECHANICAL ENGINEERING

ABCM Brazilian Society of Mechanical Sciences and Engineering
27th ABCM International Congress of Mechanical Engineering
December 04-08, 2023, Florianópolis-SC, Brazil

COB-2023-0950
EXPERIMENTAL STUDY AND ANALYSIS OF THE ENERGY PERFORMANCE OF A VAPOR COMPRESSION REFRIGERATOR POWERED BY SOLAR PHOTOVOLTAIC ENERGY FOR REGIONS WITHOUT ELECTRIFICATION

Davi S. Lopes
Willian Moreira Duarte
Luiz Machado
Beatriz de Almeida F. Bambirra Alves
Raphael Nunes de Oliveira
Universidade Federal de Minas Gerais, Belo Horizonte - MG, Brasil.
engdavisevero@gmail.com; willian@demec.ufmg.br; luizm@ufmg.br; beatrizbambirra@ufmg.br; rphnunes@demec.ufmg.br

Abstract. *In regions with less assistance and without electrification, the absence of refrigeration systems for storing vaccines, medicines and foodstuffs was evident during the Covid-19 pandemic. To supply these demands, an alternative, in line with sustainable prerogatives, would be the use of a conventional vapor compression refrigerator operating with electricity generated in a photovoltaic panel (PVC). The objective of this work was the experimental determination of the overall coefficient of performance (COP) of a commercial refrigerator with a volume of 79 L associated with a photovoltaic panel with a power of 320 W and an efficiency of 19%. In addition to these components, the experimental bench had an MPPT charge controller, an AC-DC converter with 90% efficiency and two electric batteries with unit loads of 45 Ah. To obtain the refrigerator COP, an electrical resistor was placed into internal compartment. The resistor was supplied with electric current by a variable voltage source, which provided a dissipated power of 30 W to 70 W. In addition to this rate of internal heat generation, the input of energy from the environment to the interior of the refrigerator was obtained with the help of heat transfer correlations for natural convection and thermal radiation. These correlations and the corresponding energy balances were subsidized with values of temperature obtained by calibrated K-type thermocouples installed on the internal walls and on the coil of the refrigerator evaporator. A data acquisition system was used to record the internal temperatures and the environment. Compressor energy consumption was recorded by an energy meter, which was also connected to the data acquisition system. The results of 35 experimental tests revealed that the cooling capacity of the machine ranged from 75 W to 137 W, for which the corresponding COP values associated with the refrigeration cycle ranged from 1.05 to 1.40, while the values of the global COP ranged from 0.17 to 0.24. The energy performance of the solar refrigerator was less than that relative to standard operation, whose reference COP provided by the manufacturer is 1.45. The reason for this significant drop in efficiency was due to the combined efficiencies of the PVC, inverter, and electrical components in the system. However, the PVC refrigerator proved to be viable for use in areas without electrification, mainly in regions with high availability of solar energy.*

Keywords: *refrigerator, COP, photovoltaic panel, solar energy, renewable energy*

1. INTRODUCTION

Refrigerators are systems capable of removing heat from an internal environment and rejecting it to an external environment. Electric power is required for this process to take place. These systems are responsible for 7.8% of the total global emissions of greenhouse gases, in which 63% of them come from indirect emissions, from the energy that moves the equipment. Only when the refrigerant fluid from refrigeration systems is released into the atmosphere through leaks or poor maintenance and disposal, does their Ozone Depletion Potential (ODP) or Global Warming Potential (GWP) affect the environment. Thus, with proper maintenance and use practices, indirect impacts are largely responsible for emissions in refrigeration systems (McLinden et al., 2020). By substituting, therefore, the form and source of energy, a significant reduction in the impacts of these systems is obtained.

The electricity needed for refrigerators can be provided by photovoltaic panels, which meet the premises of sustainable development. According to Wang apud Hu et al. (2020), they have been widely used and developed due to their advantageous characteristics in which the main point is that solar energy is an inexhaustible source of energy, without generating pollution. It has also become more affordable in the last decade, with the price of kWh decreasing to less than US$ 0.05 in 2016 (China), as pointed out by Jordehi apud Hu et al. (2020), and due to the advancement of technology and economies of scale. In addition, the systems are simple, compact, have a high power-to-weight ratio and require a small skilled workforce, according to Eltawil MA, apud Modi et al. (2009). Even with the efficiencies of solar panels still

being around 15-20%, which reduces the overall COP of these systems, they are appropriate for many situations where there is good solar incidence because, in addition to the other advantages presented, the available energy is unlimited.

The systems formed by vapor compression refrigerators, operated by photovoltaic panels, can be used to meet the demand for the conservation of vaccines, medicines and food at low temperatures in some regions. This demand was more evident during the Covid-19 pandemic. Vaccination coverage as a whole is considerably affected when there is an extraordinary need for vaccination for a specific disease, as in a pandemic. The less assisted and developed regions are the ones that are most affected. In the North and Northeast of Brazil, mainly, there was a significant loss of immunization coverage for poliomyelitis. The least developed states and regions had the biggest declines (Donalisio et al., 2023). This problem in the supply of vaccines has been going on and has been fought for some years. When it is not the unavailability of the electrical network to supply the vaccine refrigeration systems, the instability of the network becomes the problem. An analysis of data from temperature change notification forms in northwest São Paulo, Brazil, from the epidemiological surveillance group of São José do Rio Preto, showed that 70.1% of the 341 notifications between 2010 and 2017 were due to structural reasons, such as lack of electricity and electrical installation problems (Patine et al., 2021)

Thus, the objective of this work is to experimentally evaluate an alternative to meet these demands in accordance with sustainable prerogatives: A vapor compression refrigerator, operated by photovoltaic solar energy. The main objective is to estimate values for the overall coefficient of performance (COP) of a refrigeration system as an electrical resistor inside it has its power ranging from 30 to 70 W. The system consists of a 79 L refrigerator associated with a 320 W photovoltaic panel and nominal efficiency of 19%. In addition to these components, the bench has two 45 Ah batteries, an 88% efficiency inverter and an MPPT charge controller. To obtain the results, correlations were used for heat transfer, internal energy balance and experimental data recorded by the acquisition system, such as internal temperatures, environment and compressor power. Considerations are also made regarding the internal temperatures, under which the vaccines/inputs would be subjected.

2. METHODOLOGY

2.1 Experimental apparatus

The experimental bench is initially formed by a 79 L vapor compression refrigerator from Eletrolux associated with a photovoltaic panel of 320W of power and nominal efficiency of 19.18%, two 45 Ah batteries (C20) and a power panel, as shown in the model in Figure 1.

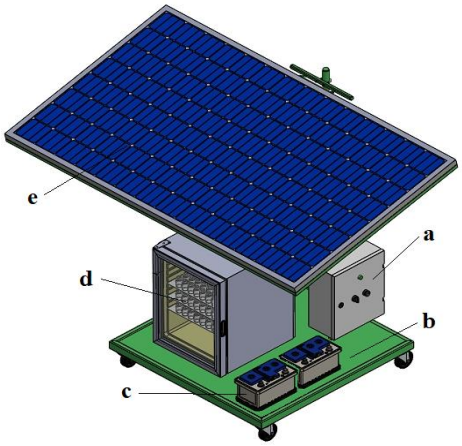

a	Panel of forces and controls
b	mobile base
c	stationary batteries
d	refrigerator
e	Photovoltaic solar panel (PV cells)

Figure 1 – Basic model of the photovoltaic solar operated refrigerator countertop

In addition to these components, an 88% efficiency inverter, an MPPT charge controller, nine K-type thermocouples, two data acquisition devices (Fieldlogger), an electrical resistor, a voltage variator for the resistor, a power panel and some electrical devices necessary for the system operation and measurements are added to the system. Figure 2 presents the actual system after assembly and Table 1 show the components.

Figure 2 - Front and side view of the refrigeration bench. Source: Own authorship (2022)

Table 1 – Components of the refrigerator countertop

Components					
Refrigerator (RE80 – Eletrolux)		**Panel photovoltaic**		**Electrical resistor**	
Storage capacity	79 L	Rated power	320 W	Maximum power	150 W
Height	64 cm	Module external area	1,67 m²	Maximum voltage	127V
Width	49,5 cm	Energy efficiency	19,18 %	**MPPT charge controller** **Fieldlogger (2)** **Type K thermocouples (9)** **Voltage variator**	
Depth	54 cm	Weight	18 kg		
Voltage	127 V	**Inversor**			
Refrigerant Gas	R134a	Power	300 W		
Stationary batteries (2)		Efficiency	88 %		
Capacity	45 Ah (C20)[1]	Voltage	Input 12VDC Output 127VAC		
Voltage	13,4 a 13,8 V				

1. 20h download time

The internal dimensions of the refrigerator are shown in Figure 3.

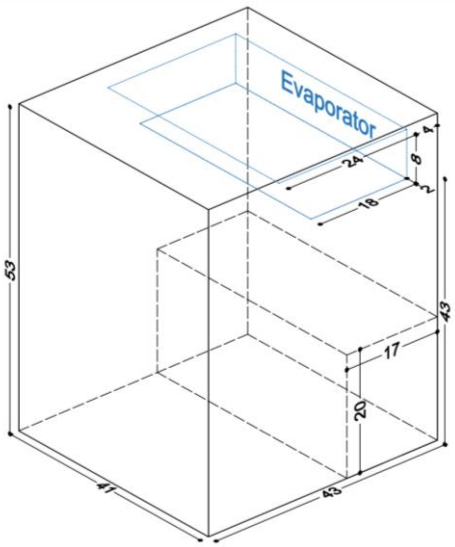

Figure 3 - Internal dimensions of the refrigerator (Own authorship)

2.2 Procedure

The refrigerator is kept in operation by two stationary batteries connected in parallel, which are charged by the photovoltaic panel. There is a charge controller interconnecting the panel, the inverter and the batteries. The inverter transmits direct current, coming from the batteries of about 12V, as alternating current of about 127V to the compressor of the refrigerator. An electrical resistor remains connected and positioned at the bottom of its interior. In the voltage variator, an appropriate voltage is defined so that the power dissipated by the resistor is as required. Initially, the power is 30W. After about 1h and 30min, the system reaches the steady state and the resistance is increased by 5W, going to 35W. This procedure of increasing the power in the resistor is repeated until reaching 70W, when the tests are finished. The tests are carried out in the morning, between 8:00 and 12:00 h, while the ambient temperature is kept close to 25°C. At all times, the two fieldloggers record internal and ambient temperatures, compressor power and electrical resistor power. The temperatures are measured at the positions as indicated in Figure 4, where it is also possible to visualize the electrical resistor.

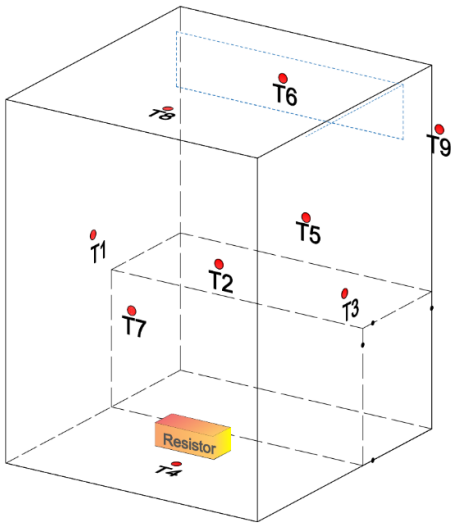

Thermocouple	Position
T1	Right side wall
T2	Center cooler (air)
T3	Left side wall
T4	Floor
T5	Back wall
T6	Evaporator
T7	Door
T8	Ceiling
T9	Room temperature

Figure 4 – Thermocouples positions

The software used for monitoring and recording data from the acquirers is the FieldLogger V1.6.9.03 Configurator, supplied by the device manufacturer. In Figure 5, it is possible to see the display of data monitoring by the software, such

as temperatures, power in the inverter and power in the electrical resistor (dark orange line where you can see the 5W steps).

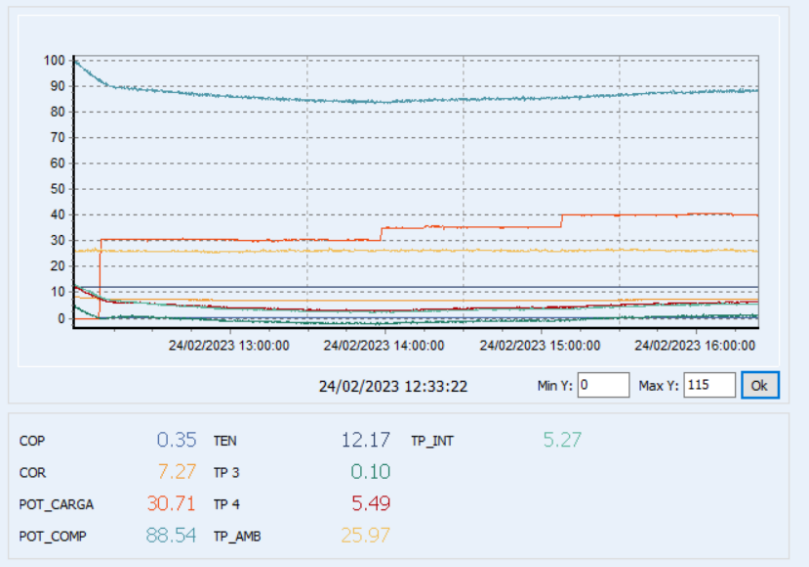

Figure 5 - Data monitoring by FielLogger Config V1.6.9.03

After the tests are finished, the collected data are handled and organized in Microsoft Excel, where the measurements and uncertainties of the thermocouples are also adjusted according to their calibration certificates. All equations using correlations and expressions for heat transfer are done in the Engineering Equation Solver (EES).

The 300W inverter used does not have the capacity to start the compressor, so a complementary system connected to the mains voltage source is used to start it. After activating the compressor, the refrigerator is then connected to the described system and the measurement procedure is carried out.

2.3 Modeling

2.3.1 Internal energy balance

There is a rate of heat that enters the internal compartment of the refrigerator due to the thermal insulation not being perfect. Condensers are located on the side walls, which is a contributing factor to this heat input. Heat dissipates internally among its three basic forms of transfer. It is possible to make an energy balance, according to the scheme in Figure 6, similar to that presented by Alqaisy et al. (2021). In this particular case, the heat conduction between the refrigerator and the ceiling is added, which proves to be significant. Thus, the total heat rate that enters the refrigerator can be divided into four parts: Convection, Radiation, Conduction and the Power dissipated by the resistor. The sum of these four terms, in the steady state, is equal to the cooling capacity (estimated for each power of the electrical resistor), according to Eq. 1.

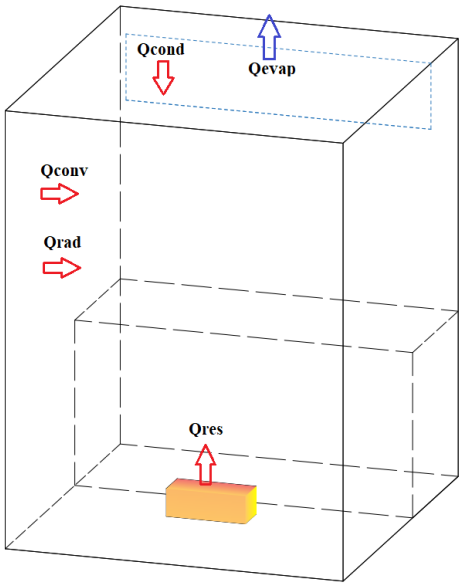

Figure 6 - Energy balance inside the refrigerator

$$\dot{Q}_{evap} = \dot{Q}_{conv} + \dot{Q}_{rad} + \dot{Q}_{cond} + \dot{Q}_{res}, \quad (1)$$

where $\dot{Q}_{evap}$ are the refrigerating capacity; $\dot{Q}_{conv}, \dot{Q}_{rad}$ *e* $\dot{Q}_{cond}$ are the rate of heat by convection, radiation and conduction, respectively, and $\dot{Q}_{res}$ the rate of heat dissipated by the resistor.

The terms referring to the heat transfer modes can be further subdivided for each region of the refrigerator: floor, side walls (right and left), door, back wall and ceiling, as follows.

2.3.2 Convection heat

For convective heat transfer, the correlations presented by Corcione (2003) are used for closed rectangular concavities heated from the sides and bottom and cooled from the top, according to Eqs. 2, 3 and 4 together with the standard deviation and errors.

$$Nu_{side} = 0.590A^{0.05}Ra^{0,15} \qquad \alpha = 0.056, \eta = 0.090 \quad (2)$$

$$Nu_{floor} = 0.182A^{0.15}Ra^{0,25} \qquad \alpha = 0.044, \eta = 0.082 \quad (3)$$

$$Nu_{ceiling} = 0.930A^{-0.30}Ra^{0,20} \qquad \alpha = 0.029, \eta = 0.058, \quad (4)$$

where A is aspect ratio of the enclosure in the range, Ra is the number of Rayleigh and α and η are the standard deviation of data and the absolute value of the maximum relative error, respectively.

These equations are used based on the model in Figure 7, where the Th used is the arithmetic mean of the temperatures measured on the walls, floor and door, which are very close to each other. The temperature Tc is that of the evaporator. Furthermore, the considered width L is the average between the real dimensions of the base (43 and 41).

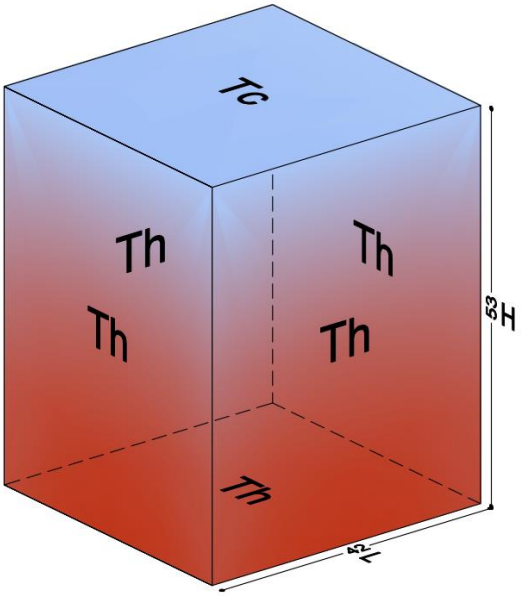

Figure 7 - Physical model for convection

This model served as the basis for applying the correlations and consequent determination of the Nusselt and convection coefficient, obtained by Eq. 5. However, the heat rate was obtained considering the real areas of each region, used in Equation 6. For the roof heat convection, the lower area of the evaporator was considered.

$$Nu = hH/k, \tag{5}$$

where h, H and k are the heat transfer coefficient, height of the concavity and the thermal conductivity of air at film temperature.

$$\dot{Q}_{conv} = h_i A_i (Th - Tc), \tag{6}$$

where i is the region to be considered and A the area.

2.3.3 Radiation heat

Radiant heat transfer between each region and the evaporator is determined from Equation 7, presented by Cengel.

$$Q_{12} = \sigma\,(T_1^4 - T_2^4) \,/\, [\,(1 - \varepsilon_1)/(A_1\,\varepsilon_1) + 1/A_1F_{12} + (1 - \varepsilon_2)/(A_2\,\varepsilon_2)], \tag{7}$$

where the indices 1 and 2 are for the hot and cold surface, respectively, and σ, ε and F are Stefan-Boltzmann constant, the emissivity of the surface - 0.90 for white paint (Çengel, Yunus A., 2013) - and the form factor, respectively.

3. RESULTS AND DISCUSSIONS

3.1 Temperatures

For each resistor power, an average is obtained for the recorded temperatures, shown in Table 2.

Table 2 - Indoor and ambient temperatures

Resistor Power	Temperatures								
	Right wall	Left wall	Floor	Door	Back	Ceiling	Air (center)	Evaporator	Ambient
30	1.15	1.7	3.9	2.47	-1.2	5.4	-3.45	-19.14	25.35
35	3.63	4.34	6.68	5.08	0.8	6.3	-0.89	-17.36	27.56

40	6.42	7.2	9.91	8.33	3.48	8.6	2.2	-15.53	27.88
45	7.77	8.78	11.22	9.29	3.7	9.8	3.51	-14.45	27.57
50	8.02	8.7	10.22	9.8	3.8	11.03	3.17	-15.36	25.57
55	12.25	13.27	15.09	14.27	7.26	15.58	7.4	-12.33	25.99
60	14.06	15	14.98	14.36	7.27	15.48	8.99	-11.06	26.12
65	15.36	16.38	18.6	17.75	9.84	18.8	10.31	-11.73	25.87
70	18.33	19.42	22.17	21.14	12.29	21.91	13.16	-9.85	25.97

The power of the resistor simulates conditions where the evaporation temperature would be higher, starting at -19.14 and reaching -9.85 °C. The temperatures in the center of the refrigerator (-3.45 to 13.16), under which the vaccines would be subjected, encompass the appropriate refrigeration range for them, from 2 to 8 °C. As for these refrigeration temperatures, the positioning inside the refrigerator must also be considered. From the center towards the walls, the temperature increases by a few degrees Celsius. This behavior is shown by Corcione (2003), Figure 9, by means of isothermal lines as a function of the ratio A between the width and height of the concavity.

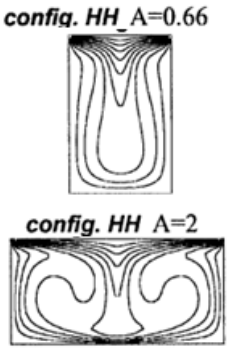

Figure 8 - Isotherms inside a rectangular concavity heated at the sides and cooled at the top, for a ratio between width and height (A) of 0.66 and 2.

The ratio for the refrigerator in this work is A=0.42/0.53=0.81, approaching the first situation where A=0.66.

3.2 Heat

The heat rates found for each internal region and transfer mode are presented in Table 3.

Table 3 - Internal heat transfer according to each region and transfer mode

Potência resistor [W]	**Transferência de calor [W]**									
	Parede direita				**Parede esquerda**				**Piso**	
	Conv	Rad1	Rad2	Rad3	Conv	Rad1	Rad2	Rad3	Conv	Rad
30	2.00	1.41	0.61	0.45	2.00	1.45	0.63	0.47	4.08	1.90
35	2.10	1.50	0.65	0.48	2.10	1.55	0.67	0.50	4.28	2.03
40	2.22	1.61	0.70	0.52	2.22	1.67	0.72	0.54	4.53	2.21
45	2.25	1.65	0.72	0.53	2.25	1.73	0.75	0.56	4.58	2.26
50	2.34	1.73	0.75	0.56	2.34	1.78	0.77	0.57	4.79	2.23
55	2.49	1.89	0.82	0.61	2.49	1.98	0.86	0.64	5.08	2.49
60	2.43	1.96	0.85	0.63	2.43	2.05	0.89	0.66	4.95	2.38
65	2.81	2.13	0.92	0.69	2.81	2.22	0.96	0.72	5.78	2.82

70	2.95	2,27	0.99	0.73	2.95	2.37	1.03	0.76	6.08	3.07
Potência Resistor [W]	**Porta**			**Trás**				**Teto**		
	Conv	Rad1	Rad2	Conv	Rad1	Rad2	Cond	Conv	Cond	Rad
30	2.31	0.86	0.45	2.30	1.39	1.79	0.32	8.59	2.58	9.40
35	2.42	0.92	0.47	2.42	1.43	1.85	0.33	9.02	2.51	9.20
40	2.56	1.01	0.52	2.55	1.54	1.99	0.35	9.53	2.57	9.60
45	2.59	1.01	0.52	2.58	1.48	1.91	0.33	9.64	2.60	9.78
50	2.70	1.07	0.55	2.69	1.56	2.01	0.35	10.05	2.82	10.66
55	2.87	1.18	0.61	2.86	1.65	2.13	0.36	10.69	3.02	11.76
60	2.80	1.14	0.59	2.80	1.56	2.01	0.34	10.43	2.88	11.25
65	3.24	1.34	0.69	3.23	1.85	2.39	0.40	12.11	3.32	13.14
70	3.41	1.45	0.75	3.40	1.94	2.51	0.41	12.73	3.48	14.04

Some heat rates were not very significant, mainly the conduction between the back region and the roof.

3.3 Coefficient of performance (COP)

Adding the heat rates previously found for each power of the electrical resistor, we obtain, by Equation 1, the cooling capacity. The COP is then obtained by Equation 8 and the global COP is obtained considering the combined efficiencies of the inverter and photovoltaic panel, according to Equation 9. These parameters are presented in Table 4, together with the compressor power.

$$COP = \dot{W}_c / \dot{Q}_{evap}, \tag{8}$$

where $\dot{W}_c$ is the power in the compressor, measured by the Fieldlogger.

$$COP_{global} = COP\ x\ n_{inv}\ x\ n_{pv}, \tag{9}$$

where, n_{inv} and n_{pv} are the efficiencies of the inverter and solar panel respectively.

Table 4 - Cooling capacity, compressor power, chiller COP and overall COP

Potência Resistor [W]	$\dot{Q}_{evap}$	$\dot{W}_c$	COP	COP_{global}
30	75.00	71.58	1.05	0.177
35	81.44	75.86	1.07	0.181
40	89.14	80.43	1.11	0.187
45	94.70	82.32	1.15	0.194
50	102.31	78.87	1.30	0.219
55	111.48	87.43	1.28	0.215
60	115.03	90.43	1.27	0.215
65	128.57	92.35	1.39	0.235
70	137.33	98.09	1.40	0.236

COP values associated with the refrigeration cycle ranged from 1.05 to 1.40. The energy performance of the solar refrigerator was lower than that normally obtained for standard vapor compression refrigeration systems, whose COP is between 2 and 4 for domestic refrigerators. Global COP values ranged from 0.18 to 0.24. These are even smaller as the combined efficiency of the PVC and the inverter is considered.

4. CONCLUSION

This work evaluated the energy performance, through COP, of a vapor compression refrigerator operated by photovoltaic solar energy. The refrigeration system would be an alternative to meet the demand for refrigerators to store vaccines, medicines and supplies in regions without electrification.

As the power of the electrical resistor inside the refrigerator dissipated from 30 to 70 W, the internal temperature (of the air in the center) varied between -3.45 to 13.16 °C, the refrigeration capacity varied from 75 W to 137.33 W, the Refrigerator COP from 1.05 to 1.40 and the global COP from 0.177 to 0.238. During the tests, the average ambient temperature fluctuated around 26°C.

The energy performance of the refrigerator was lower than that normally obtained for standard vapor compression refrigeration systems, whose COP is between 2 and 4 for domestic refrigerators. However, due to the availability of solar energy and current accessibility to systems and equipment for photovoltaic solar refrigeration, this it constitutes a viable alternative to the need presented.

5. REFERENCES

Alqaisy, S.J., Hmood, K.S., Aboaltabooq, M.H.K., Apostol, V., Pop, H., Douri, J.A., Bădescu, V., 2021. Experimental COP evaluation of a 65-litre household refrigerator running with R600a. E3S Web Conf. 286, 01008. https://doi.org/10.1051/e3sconf/202128601008

Çengel, Yunus A., M.A.B., 2013. Termodinâmica, 7th ed. AMGH, Porto Alegre.

Corcione, M., 2003. Effects of the thermal boundary conditions at the sidewalls upon natural convection in rectangular enclosures heated from below and cooled from above. International Journal of Thermal Sciences 42, 199–208. https://doi.org/10.1016/S1290-0729(02)00019-4

Donalisio, M.R., Boing, A.C., Sato, A.P.S., Martinez, E.Z., Xavier, M.O., Almeida, R.L.F. de, Moreira, R. da S., Queiroz, R.C. de S., Matijasevich, A., 2023. Vacinação contra poliomielite no Brasil de 2011 a 2021: sucessos, reveses e desafios futuros. Ciênc. saúde coletiva 28, 337–337. https://doi.org/10.1590/1413-81232023282.17842022

Hu, T., Liu, J., Hao, Z., Chang, J., 2020. Design and experimental study of a solar compression refrigeration apparatus (SCRA) for embankment engineering in permafrost regions. Transportation Geotechnics 22, 100311. https://doi.org/10.1016/j.trgeo.2019.100311

McLinden, M.O., Seeton, C.J., Pearson, A., 2020. New refrigerants and system configurations for vapor-compression refrigeration. Science 370, 791–796. https://doi.org/10.1126/science.abe3692

Modi, A., Chaudhuri, A., Vijay, B., Mathur, J., 2009. Performance analysis of a solar photovoltaic operated domestic refrigerator. Applied Energy 86, 2583–2591. https://doi.org/10.1016/j.apenergy.2009.04.037

Patine, F. dos S., Lourenção, L.G., Wysocki, A.D., Santos, M. de L.S.G., Rodrigues, I.C., Vendramini, S.H.F., 2021. Análise da perda de vacinas por alteração de temperatura. Rev. Bras. Enferm. 74, e20190762.

6. RESPONSIBILITY NOTICE

The authors are solely responsible for the printed material included in this work.